Albacore: A Sub Drone for Shallow Waters
A preliminary study

Enrico Petritoli, Fabio Leccese
Science Department, Università degli Studi "Roma Tre"
Via Della Vasca Navale n°84, 00146
Rome, Italy
e_petritoli@libero.it - ORCID: 0000-0002-6135-8386
fabio.leccese@uniroma3.it - ORCID: 0000-0002-8152-2112

***Abstract*—In this paper the idea to develop an underwater drone optimized for shallow water, inland ports and small inlets is shown. The vehicle should be simple and robust: a mathematical part is included on the vertical balance to be able to size weights and payload volumes.**

Keywords - AUV; Drone; Shallow; Water.

I. Introduction

This paper is part of several preliminary studies by Underwater Drones Group (UDG) of the Science Department of the Università degli Studi "Roma Tre", which is developing a series of advanced Autonomous Underwater Vehicles (AUVs) for the exploration of the sea at high depths. The final aim of the general project is to create several platforms for underwater scientific research that can accommodate a wide range of different payloads optimized for the most usual tasks [1]-[12]. The underwater vehicle was named *Albacore* (*Thunnus Alalunga*) due to the extreme similarity in both size and shape with the tuna well widespread in the Mediterranean: it was designed for use in shallow, high turbulence waters, often in the presence of natural obstacles (rocks and shoals) but also wrecks or breakwaters, etc. For all this reasons, it has been equipped with two powerful engines that operate counter-rotating propellers and an elliptical wing, sturdy and stiff [13]-[18].

II. The Vehicle

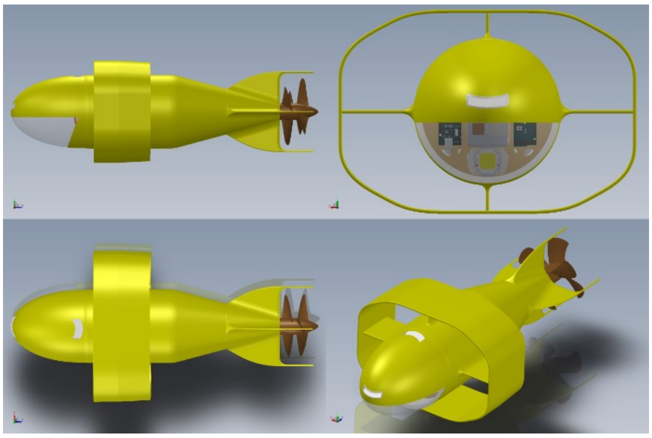

Figure 1. Four views of the AUV Albacore.

The vehicle is a cylindrical AUV, with an annular wing and propelled by a double electric motor. Let's look at its detailed description (see Figure 1).

A. The Fuselage

The fuselage of the Albacore (see Figure 2) is roughly cylindrical, composed of milled aluminium 6061 class: in the front, we have an elliptical radome act to contain the payload that consists on several biochemical sensors arranged in a "nostril" that has the purpose of protecting the instrumentation without exposing it directly to the outside [19]-[27].

In the lower section, there is a transparent porthole in polymethylmethacrylate (Plexiglas): it is the window for the camera (GoPro class) and the relative lighting system.

The central part supports the supports of the elliptical wing and is further stiffened by a series of internal battens. The terminal cone (this too stiffened in the same way) supports the fletching and the thrust of two counter-rotating propellers [28]-[35].

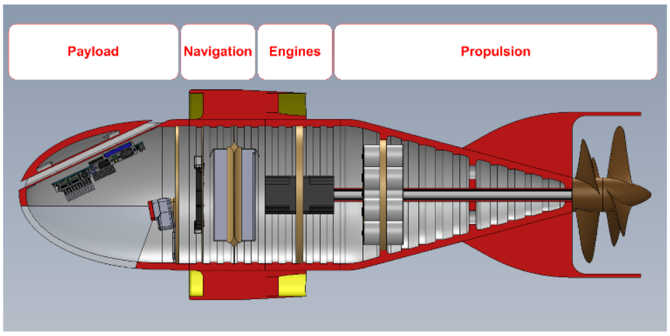

Figure 2. Cross section of the AUV Albacore: the interior arrangement of the vehicle is visible.

The fuselage is composed by four coaxial cylindrical compartments (or bays):

- Payload bay
- Navigation bay
- Engines bay and
- Propulsion bay.

B. Payload Bay

The Payload Bay is, in essence, a "radome", which contains the "nostril" (see Figure 3) whose channel in turn houses the chemical and biological sensors: the data collected are managed by a PC-104 computer card, which also has the task of sending them to the central computer (Arduino) [36]-[42]. The nostril is inclined of 20° so that its flow is the least disturbed possible and its discharge flow does not create turbulence or disturbance to the flow of the elliptical wing. Below, there is the corresponding window of a digital camera

(Go-Pro class): in anticipation of its use for visual inspection and automatic recognition of objects at depths, which, although modest, could be lacking in sufficient light, on the bulkhead will be mounted a 10^6 candle, flat LED. Lighting for the camera is important in the case of operation in the low waters of the ports, notoriously turbid or in co-current sources coming from silty river mouths [43]-[46].

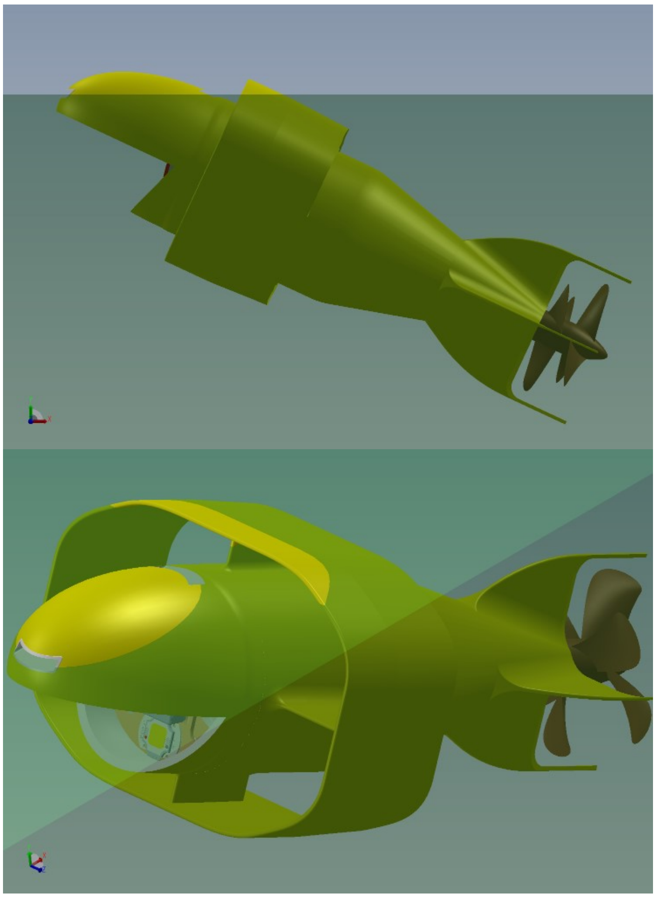

Figure 3. The drone in "nose up" attitude (upper) side view; (lower) prospective view.

C. Navigation Bay

The Navigation Bay contains two Arduino units: due to their quality level COTS (Commercial Off-The-Shelf), it was decided to put them in Main and Redundant configuration. The second unit (redundant) is placed in "hot strand by", that is to say, despite being fed and while managing the same data flow, it is not called to play the role of OBDH (On Board Computer and Data Handling) as instead the Main Unit does: this allows, in the event of a malfunction, to take over the latter in a completely transparent manner to the rest of the devices to which they are interfaced (see Figure 4). The bay also contains the two main rechargeable batteries: one supplies power to the ODBH and the other to the payload. The differentiation was necessary due to the fact that, in the event of a serious failure of the first battery, the second, disconnecting all non-essential services, can supply the energy needed by the Arduino computer to be able to lead the vehicle to the surface and to manage any recovery procedures.

D. Engines Bay

The engine bay contains two identical but counter-rotating electric motors (CW and CCW) which in turn operate the two propellers, also these counter-rotating. The movement is transmitted by two concentric drive shafts: the first (CW) is internal and moves the propeller at the end, the second (CCW) is hollow and allows the rotation of the first and moves the propeller closer to the hull. Due to the length of the drive shafts, two bearings were placed to attenuate any vibrations, one at the auxiliary battery cluster and another near the tail.

E. Propulsion Bay

The propulsion bay contains first and foremost the battery cluster, the drive shafts of the engines, the fletching and the two counter-rotating propellers. The battery cluster is composed of a canister that supports 12 "D" type accumulators of a completely different technology compared to the two main batteries so that, given the same environment, it has a completely different reliability (electromechanical degradation) response. Thanks to a small engine, it is possible to slide the chassis backwards so that the centre of mass of the vehicle moves quite far from the hydrostatic centre and so the hull can assume the "nose up" position for biochemical measurements (see Fig. 4).

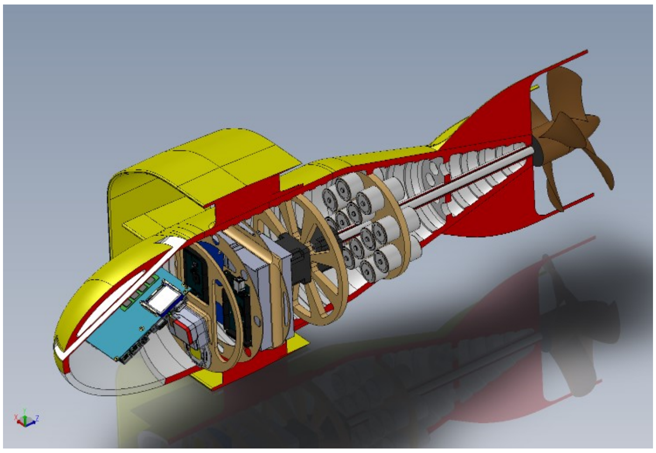

Figure 4. Prospective cross section of the AUV Albacore: the interior sections and supports are visible.

The cruciform flutes have no dihedral and have been prolonged to act as a guard for the propellers, thus preventing them from being sized in the presence of tufts of algae or wandering nets. Finally, the propellers are counter-rotating in order to counteract the strong torque of the engines, which are especially slow-moving because we are in the absence of a large wingspan that can counteract them. The terminal propeller has an angle of attack greater than the previous one in order to have the same performance as the previous one, being lapped by a flow already in rotation.

F. The Wing

Following a careful study, an elliptical annular wing was chosen for the vehicle: the peculiarity of the configuration was dictated by very strict requirements. First of all, with this solution we have practically halved the wingspan, greatly reducing the moment of inertia on the longitudinal axis: this apparent "introduction of instability" is largely compensated for the presence of spoilers that guarantee the vehicle's dynamic stability. One of the possible applications of the AUV is that of the underwater inspection of fishing nets, submerged systems and submarine cables: the fact of having a ring-shaped wing guarantees the fact that it does not get caught in possible underwater obstacles [47]-[50].

Among the main requirements, it was considered that the vehicle can be used by unskilled personnel with equipment not specially adapted: it will be sufficient, therefore, to be able to set sail on board, to have a simple winch: in this case the wing has been strengthened to operate as a "bumper" and withstand without damage possible minor bumps against the ship's rail. Last but not least, the elliptical annular wing gives the vehicle great dynamic stability, a modest induced resistance, a dimensional compactness: this is supported by four cross-shaped bracing that also act as a further element of stability.

III. Dynamic Force Balance

In this section, we consider the drone emerging at constant speed (see Fig. 5).

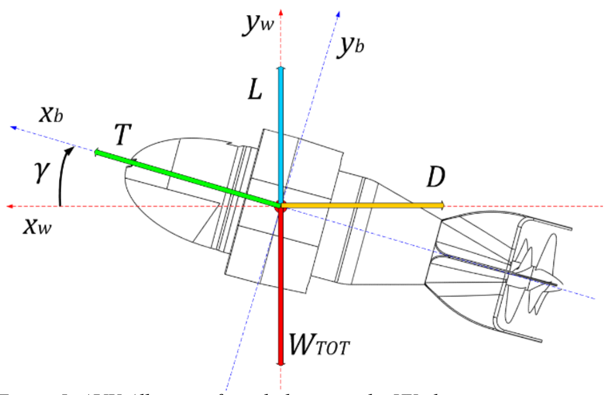

Figure 5. AUV Albacore: force balance on the XY plane.

At the equilibrium, the dynamic on the x_w and y_w axis are, at constant speed:

$$\begin{cases} 0 = T\cos\gamma - D \\ 0 = T\sin\gamma + L - W_{tot} \end{cases} \tag{1}$$

Where

T : thrust

D : drag due to the shape of the vehicle

v : drone relative speed (refer to water)

L : lift

γ : angle of attack

W_{tot} : total weight

The complete expression for the *drag* is:

$$D = \frac{1}{2}\rho v^2 S C_D \tag{2}$$

where:

ρ : seawater density (average 1.025 kg/L)

S : drone wing surface

v : drone relative speed (refer to water)

C_D : coefficient of drag

According to Taylor method [51], the last member can be separated in:

$$C_D = C_{D_0} + C_{D_\gamma}\gamma \tag{3}$$

where:

C_{D_0} : coefficient of drag at $\gamma = 0$

C_{D_γ} : coefficient of drag at $\gamma \neq 0$

so the (2) becomes:

$$D = \frac{1}{2}\rho v^2 S\left(C_{D_0} + C_{D_\gamma}\gamma\right) \tag{4}$$

The expression for the *lift* is:

$$L = \frac{1}{2}\rho v^2 S C_L \tag{5}$$

where:

C_L : coefficient of lift

According to Taylor method as per Eq. (3):

$$C_L = C_{L_0} + C_{L_\gamma}\gamma \tag{6}$$

where:

C_{L_0} : coefficient of lift at $\gamma = 0$

C_{L_γ} : coefficient of lift at $\gamma \neq 0$

so the (5) becomes:

$$L = \frac{1}{2}\rho v^2 S\left(C_{L_0} + C_{L_\gamma}\gamma\right) \tag{7}$$

For the weight we have

$$W_{tot} = W_{DW} - B_{GB} \tag{8}$$

where

W_{DW} : dry weight of the drone

B_{GB} : buoyancy of the drone

so, for the (1) we have:

$$\begin{cases} 0 = T\cos\gamma - \frac{1}{2}\rho v^2 S\left(C_{D_0} + C_{D_\gamma}\gamma\right) \\ 0 = T\sin\gamma + \frac{1}{2}\rho v^2 S\left(C_{L_0} + C_{L_\gamma}\gamma\right) - W_{DW} + B_{GB} \end{cases} \tag{9}$$

Now we evidence the thrust:

$$\begin{cases} T\cos\gamma = +\frac{1}{2}\rho v^2 S\left(C_{D_0} + C_{D_\gamma}\gamma\right) \\ T\sin\gamma = -\frac{1}{2}\rho v^2 S\left(C_{L_0} + C_{L_\gamma}\gamma\right) + W_{DW} - B_{GB} \end{cases} \tag{10}$$

so:

$$\begin{cases} T = \dfrac{+\frac{1}{2}\rho v^2 S\left(C_{D_0} + C_{D_\gamma}\gamma\right)}{\cos\gamma} \\ T = \dfrac{-\frac{1}{2}\rho v^2 S\left(C_{L_0} + C_{L_\gamma}\gamma\right) + W_{DW} - B_{GB}}{\sin\gamma} \end{cases} \tag{11}$$

Upper and lower member are the same, so:

$$\frac{+\frac{1}{2}\rho v^2 S\left(C_{D_0} + C_{D_\gamma}\gamma\right)}{\cos\gamma} = \frac{-\frac{1}{2}\rho v^2 S\left(C_{L_0} + C_{L_\gamma}\gamma\right) + W_{DW} - B_{GB}}{\sin\gamma} \tag{12}$$

Now, in order to isolate the angle of attack:

$$\frac{\sin\gamma}{\cos\gamma} = \frac{-\frac{1}{2}\rho v^2 S\left(C_{L_0} + C_{L_\gamma}\gamma\right) + W_{DW} - B_{GB}}{+\frac{1}{2}\rho v^2 S\left(C_{D_0} + C_{D_\gamma}\gamma\right)} \tag{13}$$

Then

$$\tan\gamma = \frac{-\frac{1}{2}\rho v^2 S\left(C_{L_0} + C_{L_\gamma}\gamma\right) + W_{DW} - B_{GB}}{+\frac{1}{2}\rho v^2 S\left(C_{D_0} + C_{D_\gamma}\gamma\right)} \tag{14}$$

In case of “straight and level” trajectory we have $\gamma = 0$ so

$$0 = \frac{-\frac{1}{2}\rho v^2 S C_{L_0} + W_{DW} - B_{GB}}{+\frac{1}{2}\rho v^2 S C_{D_0}} \tag{15}$$

and

$$0 = -\frac{1}{2}\rho v^2 S C_{L_0} + W_{DW} - B_{GB} \tag{16}$$

Posing

$$\kappa = \frac{1}{2}\rho S C_{L_0} \tag{17}$$

we have:

$$\kappa \cdot v^2 = W_{DW} - B_{GB} \tag{18}$$

so for the speed:

$$v = \sqrt{\frac{W_{DW} - B_{GB}}{\kappa}} \tag{19}$$

In, the graph in fig. 6, we see the trend of the function:

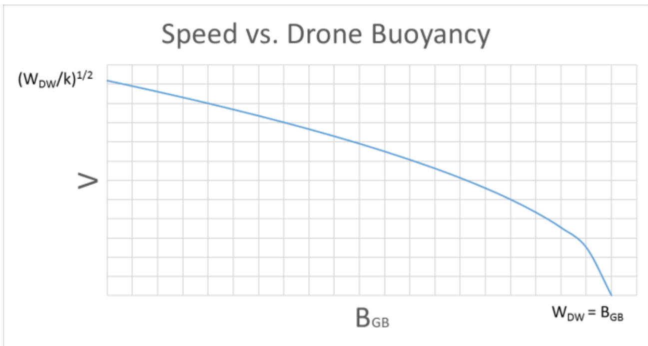

Figure 6. Qualitative trend of the function Speed vs. drone buoyancy.

The limits for v are:

$$0 < v < \sqrt{\frac{W_{DW}}{\kappa}} \tag{20}$$

the speed goes from zero to the maximum: this does not mean that the drone cannot go at higher speeds but only that it is the limit for leveled "flight". To reach higher speeds in horizontal paths it is necessary to choose negative angles of attack because the lift of the wing would bring the vehicle upwards.

The limits for B_{GB} are:

$$0 < B_{GB} < W_{DW} \tag{21}$$

The variation B_{GB} of buoyancy is obtained by means of a small external bladder which is filled and emptied of oil if necessary by means of a small electric pump. Its limits are absolutely evident: a bladder that gives a hydrostatic thrust greater than the weight itself would lead the drone to float on the surface without construct. The zero limit, on the other hand, can be overcome by appropriately ballasting the drone and obtaining a negative buoyancy: also in this case we will have that the vehicle is over ballasted and would sink directly. This type of set-up is allowed for a sub-glider but not for a classic drone.

IV. Conclusions

In this paper we have defined the general architecture for an underwater drone that is optimized for shallow water, inland ports, small inlets. The vehicle is simple and robust and divided into four main sections: Payload bay, Navigation bay, Engines bay and Propulsion bay. The study of balance on the vertical plane shows that the volume of the bladder must be well calculated otherwise it could interfere with the maximum vehicle speed.

References

[1] C. S. Draper. "Origins of inertial navigation", Journal of Guidance, Control, and Dynamics, Vol. 4, No. 5 (1981), pp. 449-463. https://doi.org/10.2514/3.19748.

[2] Woithe, H.C.; Tilkidjieva, D.; Kremer, U. Towards a resource-aware programming architecture for smart autonomous underwater vehicles; Technical Report, DCS-TR-637; Rutgers University: New Brunswick, NJ, USA, 2008.

[3] Petritoli, E., Leccese, F., Leccisi, M. Inertial navigation systems for UAV: Uncertainty and error measurements (2019) 2019 IEEE International Workshop on Metrology for AeroSpace, MetroAeroSpace 2019 - Proceedings, art. no. 8869618, pp. 218-222. DOI: 10.1109/MetroAeroSpace.2019.8869618.

[4] Hussain, N.A.A.; Ali, S.S.A.; Saad, M.N.M.; Nordin, N. Underactuated nonlinear adaptive control approach using U-model for multivariable underwater glider control parameters. In Proceedings of the 2016 IEEE International Conference on Underwater System Technology: Theory and Applications (USYS), Penang, Malaysia, 13–14 December 2016; pp. 19–25, doi:10.1109/USYS.2016.7893947.

[5] Leccese, F.; Cagnetti, M.; Giarnetti, S.; Petritoli, E.; Luisetto, I.; Tuti, S.; Đurović-Pejčev, R.; Đorđević, T.; Tomašević, A.; Bursić, V.; et al. A Simple Takagi-Sugeno Fuzzy Modelling Case Study for an Underwater Glider Control System. In Proceedings of the 2018 IEEE International Workshop on Metrology for the Sea; Learning to Measure Sea Health Parameters (MetroSea), Bari, Italy, 8–10 October 2018, pp. 262–267, doi:10.1109/MetroSea.2018.8657877.

[6] C. Jekeli “Inertial Navigation Systems with Geodetic Applications” Walter de Gruyter Berlin New York 2001.

[7] Petritoli, E.; Leccese, F.; Cagnetti, M. A High Accuracy Buoyancy System Control for an Underwater Glider. In Proceedings of the 2018 IEEE International Workshop on Metrology for the Sea; Learning to Measure Sea Health Parameters (MetroSea), Bari, Italy, 8–10 October 2018; pp. 257–261. doi:10.1109/MetroSea.2018.8657831.

[8] Lennart Ljung, “System Identification Theory for the User,” Second Edition. USA: Prentice Hall, 1999.

[9] Leonard and Graver, “Model based feedback control of autonomous underwater glider,” IEEE Journal of Oceanic Engineering, Vol. 26, No 4, pp.633-644, 2001.

[10] B. Etkin,” Dynamic of Flight,” New York and London: John Wiley and Sons, 1959.

[11] Xiaobo Tan, Drew Kim, Nathan Usher, Dan Laboy, Joel Jackson, Azra Kapetanovic, Jason Rapai, Beniamin Sabadus, Xin Zhou, "An Autonomous Robotic Fish for Mobile Sensing", Intelligent Robots and Systems 2006 IEEE/RSJ International Conference on, pp. 5424-5429, 2006.

[12] Ryan N. Smith, Arvind Pereira, Yi Chao, Peggy P. Li, David A. Caron, Burton H. Jones, Gaurav S. Sukhatme, "Autonomous Underwater Vehicle trajectory design coupled with predictive ocean models: A case study", Robotics and Automation (ICRA) 2010 IEEE International Conference on, pp. 4770-4777, 2010, ISSN 1050-4729.

[13] Smith Chao Jones Caron Li Sukhatme – “Trajectory Design for Autonomous Underwater Vehicles based on Ocean Model Predictions for Feature Tracking” Field and Service Robotics Volume 62 of the series Springer Tracts in Advanced Robotics pp 263-273.

[14] R. Austin “Unmanned Aircraft Systems” Wiley. (2010).

[15] Petritoli, E., Leccese, F. A high accuracy navigation system for a tailless underwater glider (2017) IMEKO TC19 Workshop on Metrology for the Sea, MetroSea 2017: Learning to Measure Sea Health Parameters, 2017-October, pp. 127-132.

[16] Bong-Huat Jun, Jin-Yeong Park, Fill-Youb Lee, Pan-Mook Lee, Chong-Moo Lee, Kihun Kim, Young-Kon Lim, Jun-Ho Oh. “Development of the AUV ‘ISiMI’ and free running test in an ocean engineering basin,” Ocean Engineering, v 36, n 1, pp. 2-14, January 2009

[17] Petritoli, E., Leccese, F. High accuracy attitude and navigation system for an autonomous underwater vehicle (AUV) (2018) Acta IMEKO, 7 (2), pp. 3-9. DOI: 10.21014/acta_imeko.v7i2.535.

[18] M. Arima, N. Ichihashi, T. Ikebuchi, “Motion characteristics of an underwater glider with independently controllable main wings,”OCEAN ’08 MTS/IEEE Kobe-Techno-Ocean’08-Voyage toward Future, OTO’08, 2008.

[19] Roger E.O, Genderson JG, Smith W.S, Denny G.F, Farley P.J., “Underwater acoustic glider,” Geoscience and Remote Sensing Symposium, IGARSS ’04. Proceedings. IEEE International Vol. 3, pp. 2241-2244, 2004.

[20] H. C. Woithe, Ulrich Kremer, "A programming architecture for smart autonomous underwater vehicles", Intelligent Robots and Systems 2009. IROS 2009. IEEE/RSJ International Conference on, pp. 4433-4438, 2009.

[21] H. C. Woithe, Denitsa Tilkidjieva, Ulrich Kremer, “Towards a resource-aware programming architecture for smart autonomous underwater vehicles,” Technical Report, DCS-TR-637, Dept. of Computer Science, Rutgers Univ.

[22] John F. Gardner, “Simulation of Machines, Using MATLAB and Simulink,” Canada: Wadsworth Group, 2001.

[23] Daniel L. Rudnick, Russ E. Davis, David M. Fratantoni, Mary Jane Perry, “Underwater Gliders for Ocean Research,” Marine Technology Society Journal, v 38, n 2, pp 73-84, Summer 2004.

[24] Laszlo Techy, Kristi A. Morganseny, Craig A. Woolseyz, "Long-baseline acoustic localization of the Seaglider underwater glider", American Control Conference (ACC) 2011, pp. 3990-3995, 2011, ISSN 2378-5861.

[25] Nur Afande Ali Hussain, Syed Saad Azhar Ali, Mohamad Naufal Mohamad Saad, Nadira Nordin, "Underactuated nonlinear adaptive control approach using U-model for multivariable underwater glider control parameters", Underwater System Technology: Theory and Applications (USYS) IEEE International Conference on, pp. 19-25, 2016.

[26] Pengyao Yu, Yong Zhao, Tianlin Wang, Han Zhou, Shaojuan Su, Chunbo Zhen, "Steady-state spiral motion simulation and turning speed analysis of an underwater glider", Information Cybernetics and Computational Social Systems (ICCSS) 2017 4th International Conference on, pp. 372-377, 2017.

[27] Tony Bloch, P.S. Krishnaprasad, Naomi Leonard, Richard Murray, "Jerrold Eldon Marsden [Obituaries]", Control Systems IEEE, vol. 31, pp. 105-108, 2011, ISSN 1066-033X.

[28] C.D. Williams, "AUV systems research at the NRC-IOT: an update", Underwater Technology 2004. UT '04. 2004 International Symposium on, pp. 59-73, 2004.

[29] Adamo, Francesco; Andria, Gregorio; Di Nisio, Attilio; Calò Carducci, Carlo Guarnieri; Lay-Ekuakille, Aimé; Mattencini, Giuseppe; Spadavecchia, Maurizio “Designing And Prototyping A Sensors Head For Test And Certification Of Uav Components” International Journal on Smart Sensing & Intelligent Systems . Sep2017, Vol. 10 Issue 3, p646-672. 27p.

[30] Petritoli, E., Leccese, F., Ciani, L. Reliability assessment of UAV systems (2017) 4th IEEE International Workshop on Metrology for AeroSpace, MetroAeroSpace 2017 - Proceedings, art. no. 7999577, pp. 266-270. DOI: 10.1109/MetroAeroSpace.2017.7999577.

[31] Pasquali, V., D'Alessandro, G., Gualtieri, R., Leccese, F. A new data logger based on Raspberry-Pi for Arctic Notostraca locomotion investigations (2017) Measurement: Journal of the International Measurement Confederation, 110, pp. 249-256. DOI: 10.1016/j.measurement.2017.07.004

[32] Leccese, F., Cagnetti, M., Di Pasquale, S., Giarnetti, S., Caciotta, M. A new power quality instrument based on raspberry-pi (2016) Electronics (Switzerland), 5 (4), art. no. 64, . DOI: 10.3390/electronics5040064

[33] Pasquali, V., Gualtieri, R., D'Alessandro, G., Leccese, F., Cagnetti, M. Experimental in field reliability test for data logger based on Raspberry-Pi for extreme scenarios: A first step versus aerospace applications (2016) 3rd IEEE International Workshop on Metrology for Aerospace, MetroAeroSpace 2016 - Proceedings, art. no. 7573242, pp. 365-370. DOI: 10.1109/MetroAeroSpace.2016.7573242.

[34] Pasquali, V., Gualtieri, R., D’Alessandro, G., Granberg, M., Hazlerigg, D., Cagnetti, M., Leccese, F. Monitoring and analyzing of circadian and ultradian locomotor activity based on Raspberry-Pi (2016) Electronics (Switzerland), 5 (3), art. no. 58, . DOI: 10.3390/electronics5030058.

[35] Leccese, F., Cagnetti, M., Calogero, A., Trinca, D., di Pasquale, S., Giarnetti, S., Cozzella, L. A new acquisition and imaging system for environmental measurements: An experience on the Italian cultural heritage (2014) Sensors (Switzerland), 14 (5), pp. 9290-9312. DOI: 10.3390/s140509290.

[36] J. G. Graver, J. Liu, C. Woolsey et al., “Design and Analysis of an Underwater Vehicle for Controlled Gliding,” in Conference on Information Sciences and Systems (CISS), Princeton, 1998.

[37] H. Stommel “The Slocum Mission” Oceanography, pp. 22 - 25, April 1989

[38] J.G. Graver. Underwater Gliders: Dynamics, Control and Design. PhD thesis, Princeton University, 2005.

[39] Sherman, J., R. E. Davis, W. B. Owens, and J. Valdes, 2001: The autonomous underwater glider “Spray”. IEEE J Oceanic Eng. 26:437-446.

[40] D. L. Rudnick, R. E. Davis, C.C. Eriksen et al., “Underwater Gliders for Ocean Research,” Marine Technology Society Journal, vol. 38, no. 1, Spring, 2004.

[41] A. Pereira, H. Heidarsson, D.A. Caron, B.H. Jones, and G.S. Sukhatme. An implementation of a communication framework for the cost-effective operation of slocum gliders in coastal regions. In Proceedings of The 7th International Conference on Field and Service Robotics, Cambridge, MA, July, 2009.

[42] Y.C. Lee, D.G. O’Laughlin “A Performance Analysis of a Tightly Coupled GPS INS For two integrity monitoring Methods” The MITRE Corporation, Center for Advanced Aviation System Development (CAASD).

[43] D. Küchemann “The Aerodynamic Design of Aircraft” Pergamon international library of science, technology, engineering, and social studies, 1978. Oxford: Pergamon Press. ISBN 0-08-020515-1.

[44] D. Meyer “Glider Technology for Ocean Observations: A Review” Ocean Sci. Discuss., doi: 10.5194/os-2016-40, 2016.

[45] Davis, R. E., D. C. Webb, L. A. Regier and J. Dufour. 1992. “The Autonomous Lagrangian Circulation Explorer (ALACE).” J Atmos Oceanic Technol. 9:264-285.

[46] G.Parthasarathy, Degala Shravya Sree, B.Lakshmi Manasa – “Design Mathematical Modeling and Analysis of Underwater Glider” International Journal of Science and Research (IJSR) ISSN (Online): 2319-7064.

[47] V.F. Strachan “A Review of the implications of the Johns Hopkins University Applied Physics Laboratory GPS Risk Assessment Study” Litton Aero Products, April 5th, 1999.

[48] RTCM Special Committee n.104 “RTCM Recommended standards for differential Navstar GPS Service” Ver.2.0, Jan.1, 1990.

[49] Davis, R. E., C. C. Eriksen and C. P. Jones. 2003. Autonomous buoyancy-driven underwater gliders. In: Technology and Applications of Autonomous Underwater Vehicles, ed. G. Griffiths, pp. 37-58. Taylor and Francis.

[50] Y.C. Lee, D.G. O’Laughlin “A Performance Analysis of a Tightly Coupled GPS INS For two integrity monitoring Methods” The MITRE Corporation, Center for Advanced Aviation System Development (CAASD).

[51] Warren F. Philips “Mechanics of Flight” Ed Wiley India. Ed 2009. ISBN-13: 978-8126538515